

The Effects of Nanofluids on Forced Convection Heat Transfer Inside Parallel Plate Heated with Flush Mounted Discrete Heater Sources

Ş. Ulaş Atmaca¹, İlker Göktepe², Ali Ateş³

^{1,2}Konya Technical University, Department of Mechanical Engineering, Konya, Turkey

³İlgin Vocational School, Selcuk University, Konya, Turkey

Received: 16 Jan 2023; Received in revised form: 12 Feb 2023; Accepted: 21 Feb 2023; Available online: 28 Feb 2023

©2022 The Author(s). Published by Infogain Publications. This is an open access article under the CC BY license

(<https://creativecommons.org/licenses/by/4.0/>)

Abstract— A numerical solution on forced convection of Al_2O_3 -water nanofluid for different volume fractions is investigated for laminar flow through a parallel plate with flush mounted discrete heat sources. The model used for nanofluid mixture is a single-phase approach and fluid properties are considered constant with temperature. The finite difference method is used for solutions and four different volume fractions are considered varying from 0% to 4%. A fully developed laminar velocity profile is considered and the parallel plate is assumed as heated with three discrete heat sources flush mounted to the top and bottom plate with the same lengths. Uniform wall temperature boundary condition is taken for discrete heaters. Peclet numbers are in the range of 20-100. For comparison and validity of the solution the results for a classical problem, laminar flow through a parallel plate which is heated at the downstream region with constant temperature, are obtained. Results are presented in terms of bulk temperature, heat flux, and local Nusselt number. Heat transfer is enhanced with the particle volume concentration. For comparison, pure water results are also shown in the figures. At the locations where heat is applied the heat flux values decrease as the volume fraction increase and the bulk temperature values are higher for the higher volume fractions at the heated locations. As the volume fraction increases the local Nusselt number can increase up to 30% than to pure water.

Keywords— forced convection, heat transfer enhancement, nanofluid, flush mounted discrete heating, parallel plate, numerical investigation.

I. INTRODUCTION

The classical problem of the laminar flow of fluids in the parallel plates has been investigated by many researchers for various boundary conditions. A detailed survey of these works can be found in [1]. There are also works about discrete heat sources for pipe and channel flows in literature. A comprehensive review of work on discrete heat sources in plates were presented by [2] and [3].

Two-dimensional conjugate heat transfer from flush mounted heat sources in horizontal plates numerically by [4], [5] and [6]. experimental and numerical analysis is performed by [7] to determine convection heat transfer from a single and inline four-row array of heat sources.

There are papers concerning mixed convection heat transfer from discrete heat sources [8], [9], [10], [11], [12], [13] and [3].

An innovative way to enhance the heat transfer rate in thermal equipment is using solid nanoparticles to improve the fluid thermal conductivity [14]. Nanofluids constitute base fluids and metallic or non metallic particles having size less than 100nm and are known to have better thermal conductivity than conventional fluids, [15]. A detailed review of convective heat transfer enhancement can be found in [16] and [17].

There is not much paper concerning nanofluid and discrete heat sources in the literature. According to our

acknowledgement survey, [18], [19] and [20] are the papers that can be found in the literature.

In this paper, forced convection of nanofluids (Al₂O₃-water) through two-dimensional horizontal parallel plate with discrete heat sources is investigated numerically. It is assumed as six heat sources fixed on top and bottom plate with the same length (L_h*=24) and with the same space to each other, three at bottom and three at top. The fluid assumed as enters to system with constant temperature, T_o. The discrete heaters have constant temperature of T_l. The velocity profile is considered fully developed far away from the heating region. Three different values of Peclet numbers, 20 50 and 100 are taken and Al₂O₃-water is considered as nanofluid. Four different volume fractions as 1%, 2% 3% and 4% are taken for solutions and for comparison 0% (pure water) results are given. The variation of bulk temperature, heat flux, and local Nusselt number values according to the axial position are presented graphically.

II. MATHEMATICAL MODEL

2.1. Formulation of the Problem

In the present work, a steady heat transfer problem is investigated in two-dimensional, horizontal parallel plates for thermally developing laminar flows, considering fluid axial conduction. The schematic diagram and the coordinate systems are given in Figure 1. The parallel plates are considered infinite in length and two regional. At far upstream (x*=-∞) fluid enters the channel with a uniform temperature of T_o. At the downstream of the channel, it is assumed that three discrete heaters mounted both up and down plates symmetrically which are maintaining constant wall temperature, T_l. The length of the heated and unheated locations is considered the same length. Totally six, three of them placed bottom and the other three heaters placed top plate symmetrically. The lengths of the discrete heaters are taken as L_h, and the space (unheated length) are equal to this value. Viscous dissipation is neglected at the solution of the energy equation. For the nanofluid it is assumed that;

- there is a thermal equilibrium between the base fluid (pure water) and the nanoparticles.
- the nanofluid flow is laminar and steady.
- the nanofluid is Newtonien and incompressible [19].
- the single-phase model with physical and thermal properties, all assumed to be constant with temperature. [14].

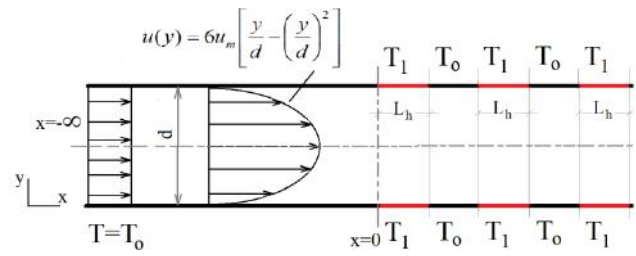


Figure 1. Schematics of the problem and the coordinate system

The fluid is water based nanofluid containing Al₂O₃ nanoparticles. The solid volume fractions, φ, have been varied between 0% to 4%. The thermophysical properties of the base fluid and nanoparticles are tabulated in Table 1.

Table 1 Properties of nanofluid [19]

Property	Water	Alumina (Al ₂ O ₃)
ρ [kg/m ³]	997.1	3970
c _p [J/kgK]	4179	765
k [W/mK]	0.613	40
μ [Pa s]	998e-6	-

The flow is assumed developed from the channel entrance. By analytical solution for the parallel plate the velocity profile is given in Eq. 1.

$$u(y) = 6u_m \left[\frac{y}{d} - \left(\frac{y}{d} \right)^2 \right] \tag{1}$$

Under these assumptions the described problem can be formulated in non-dimensional form as follows. The energy equation is

$$6Pe_{nf} (y^* - y^{*2}) \frac{\partial \theta}{\partial x^*} = \frac{\partial}{\partial x^*} \left(k^* \frac{\partial \theta}{\partial x^*} \right) + \frac{\partial}{\partial y^*} \left(k^* \frac{\partial \theta}{\partial y^*} \right) \tag{2}$$

Boundary conditions;

$$\text{at } x^* = -\infty \quad \theta = 0; \tag{3.a}$$

$$\text{at } y^* = 0.5 \quad \frac{\partial \theta}{\partial y^*} = 0; \tag{3.b}$$

$$\text{at } y^* = 0 \text{ and } y^* = 1 ; x^* > 0 \quad \theta = 1 \text{ (at wall with discrete heat sources)} \tag{3.c}$$

$$\text{at } y^* = 0 \text{ and } y^* = 1 ; x^* > 0 \quad \theta = 0 \text{ (at wall without discrete heat sources)} \tag{3.d}$$

at $y^* = 0$ and $y^* = 1$; $x^* < 0$ $\theta = 0$ (the upstream region) (3.e)

Non dimensional parameters for the problem are defined as;

$$\theta = \frac{T - T_o}{T_1 - T_o}, \quad x^* = \frac{x}{d}, \quad L_h^* = \frac{L_h}{d}, \quad y^* = \frac{y}{d},$$

$$Pe_{nf} = \frac{du_m \rho c_p}{k_{nf,b}}, \quad k^* = \frac{k_{eff,T}}{k_{eff,b}}, \quad (4)$$

Dimensionless fluid bulk temperatures, θ_b , heat flux values, q_w^* , and local Nusselt numbers, Nu , can be calculated as follows:

$$\theta_b = 6 \int_0^1 (y^* - y^{*2}) \theta_f dy^*; \quad (5)$$

$$q_w^* = - \left(\frac{\partial \theta}{\partial y^*} \right); \quad (6)$$

$$Nu = \frac{-2q_w^*}{\theta_w - \theta_b}. \quad (7)$$

2.2. Thermophysical properties of nanofluids

In the present analysis, the nanofluid flow is considered as a single phase incompressible flow. The simplest approach for the single phase assumption is the direct usage of the governing equations of pure fluid flow with the thermophysical properties of the nanofluid in consideration. [16]. Nanofluids may be considered as Newtonian fluids for low volume fractions, such as up to 10% and for small temperature increases.

The density of the nanofluid based on nanofluid volume fraction is given by [21] as follows.

$$\rho_{nf} = (1 - \varphi)\rho_f + \varphi \rho_p \quad (8)$$

For a nanoparticle liquid suspension the parameter $(\rho c_p)_{nf}$ of the nanofluid is given as [22]

$$(\rho c_p)_{nf} = (1 - \varphi)(\rho c_p)_f + \varphi(\rho c_p)_p \quad (9)$$

Nanofluid viscosity is one of the important thermophysical parameter due to its direct effect on pressure drop in forced convection. A detailed survey on viscosity of nanofluid can be found in [17] The effective dynamic viscosity of the nanofluid is given by [23] as

$$\mu_{nf} = \mu_f (1 + 39.11 \varphi + 533.9 \varphi^2) \quad (\text{for Al}_2\text{O}_3 \text{ nanoparticles}) \quad (10)$$

Many researchers suggest using nanofluids due to its higher thermal conductivity than to pure base fluid. A detailed literature review can also be found in [17]. In order to take the effect of thermal dispersion into account, the energy equation for the forced convection heat transfer of pure fluids is modified by replacing the thermal conductivity terms with an effective thermal conductivity which is defined as follows [18].

$$k_{eff} = k_{nf} + k_d \quad (11)$$

$$k_{ed} = C(\rho c_p)_{nf} u_x \phi d_p r_o \quad (12)$$

where, k_{nf} is nanofluid thermal conductivity, and k_d is called the dispersed thermal conductivity, which is proposed to be calculated by using the following expression. Here, C is an empirical constant that should be determined by matching experimental data, u_x is local flow velocity, d_p is particle diameter, and r_o is tube diameter.

2.3. Numerical Procedure

The system of equations (2) is solved by a numerical finite difference approach. Once the flow pattern is known, the heat transfer can be calculated by a numerical solution of the energy equation. The conductive terms are discretized by central difference schemes and convective term in the energy differential equation by an exact method defined in [24]. This method of discretization is a two-dimensional version of the “exact or exponential scheme” defined by [25]. The following discretization equation is obtained for an interior (non boundary) nodal point (i,j).

$$a_{i,j} \theta_{i,j} = a_{i+1,j} \theta_{i+1,j} + a_{i-1,j} \theta_{i-1,j} + a_{i,j+1} \theta_{i,j+1} + a_{i,j-1} \theta_{i,j-1} \quad (13.a)$$

where

$$a_{i+1,j} = \frac{6Pe(y_j^* - y_j^{*2})}{\exp\left[6Pe(y_j^* - y_j^{*2}) \frac{\delta x_{i+1}^*}{k^*}\right] - 1} (\Delta y_j^*); \quad (13.b)$$

$$a_{i-1,j} = 6Pe(y_j^* - y_j^{*2}) \frac{\exp\left[6Pe(y_j^* - y_j^{*2}) \frac{\delta x_{i-1}^*}{k^*}\right]}{\exp\left[6Pe(y_j^* - y_j^{*2}) \frac{\delta x_{i-1}^*}{k^*}\right] - 1} (\Delta y_j^*)$$

;

$$(13.c)$$

$$a_{i,j+1} = \frac{k^*}{\delta y_{j+1}^*} (\Delta x_i^*); \quad (13.d)$$

$$a_{i,j-1} = \frac{k^*}{\delta y_{j-1}^*} (\Delta x_i^*); \quad (13.e)$$

$$a_{i,j} = a_{i+1,j} + a_{i-1,j} + a_{i,j+1} + a_{i,j-1} \tag{13.f}$$

Due to symmetry, the solution domain is bounded between the wall and the central line of the parallel plates. Uniform grid spacing is used at solutions both in x and y directions. The optimum number for the grid system is found to be 160x60 in x and y directions respectively. Gauss-Siedel iteration technique is used for obtaining the temperature distribution. Convergence limit is taken to be 10^{-7} .

III. CODE VALIDATION

A computer code has been developed to solve the energy equation for discrete heat sources in a parallel plate. To verify the reliability of the program a solution was obtained for a classical parallel plate problem. By changing boundary conditions of classical problem, the developed program is used for discrete heating. In this classical problem, at the upstream region, the inlet temperature of the fluid is assumed as T_o . And At the downstream uniform wall temperature (T_1) boundary condition is taken. Also fully developed laminar flow is assumed for steady state problem. The schematic of the classical problem is given in Figure 2.

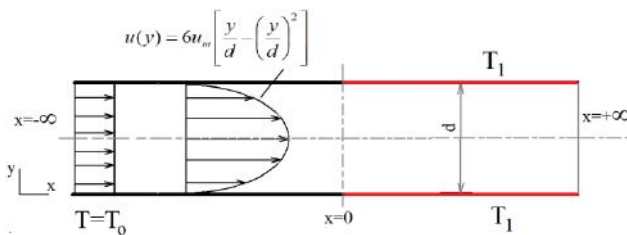


Fig.2. Schematics of the problem and the coordinate system for code validation

For fully developed laminar channel flow under constant wall boundary condition, the Nusselt number is 7.54070087 [1].The Nusselt numbers obtained by the computer program according to Peclet numbers and relative deviations from the value of 7.54070087 are given in Table 2. As can be seen from Table 2 the relative deviation between the literature and the obtained result is a maximum of 0.22 percent. It can be said that the results agree well with the literature.

Table 2. Nusselt number values for various Peclet numbers.

Peclet Number	Nusselt Number	Relative Error ϵ (%)
1	7.5396	0.015
2	7.5398	0.012
5	7.5400	0.0093

10	7.5399	0.0106
20	7.5346	0.0809
50	7.5397	0.013
100	7.5239	0.22

For the classical heat transfer problem to obtain the effect of volume fractions of nanoparticles, the axial variation of Nusselt numbers and bulk temperatures are calculated. The Nusselt number for $Pe=10$ is given in Figure 3. As can be seen from Fig.3, for small Pe number considerable amount of heat is transferred through the upstream region due to axial conduction in the fluid.

To see the effects of volume fraction of nanoparticles, the values of the local Nusselt numbers at flow direction is also given in Fig 3 for four different particle volume fractions from 1% to 4% for the same boundary condition. In these solutions, Al_2O_3 -water nanofluids are taken as the working fluids. Pure water shows the lowest local Nusselt number values. The heat transfer increases with an increase in nanoparticle concentration which is caused by the high thermal conductivity of the nanofluid. The higher local Nusselt values are obtained for pure water at the upstream region of the parallel plate. And Nusselt values decrease as volume fraction increases at the upstream region due to the higher thermal conductivity of nanofluid. This values are coincident with the results of [26].

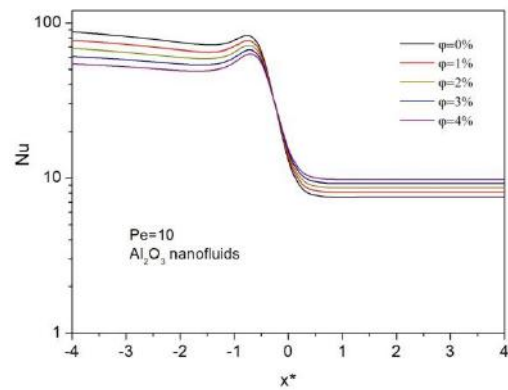


Fig.3. Axial distribution of local Nusselt number at classical heat transfer problem for $Pe=10$

For determining the effects of volume fractions of nanoparticles the bulk temperatures of the classical heat transfer problem are given. The axial bulk temperature distribution for four different volume fractions 1%,2%, 3%, and 4% is given in Figure 4. In Fig. 4.a the results are given for $Pe=50$, and Fig.4.b is for $Pe=100$. Form Fig.4 it can be seen that the thermally developing region increases as the Peclet number increases due to higher axial velocity. In Fig. it can also conclude that the effect of axial conduction could

not be seen at these ranges of Peclet numbers. Despite handling the axial conduction term in the energy equation there is not any heat penetration through the upstream region of the fluid. The effect of nanoparticles volume fraction can easily be seen at higher Peclet numbers. The lines are more distinct from each other at Fig.b.

As can be seen from Figure 4, the volume fractions of the nanoparticle do not have a significant effect on the thermal entrance lengths. The bulk temperature values are higher as the volume fraction increases due to higher thermal conductivity values. The bulk temperature gets its asymptotic value of 1 as expected.

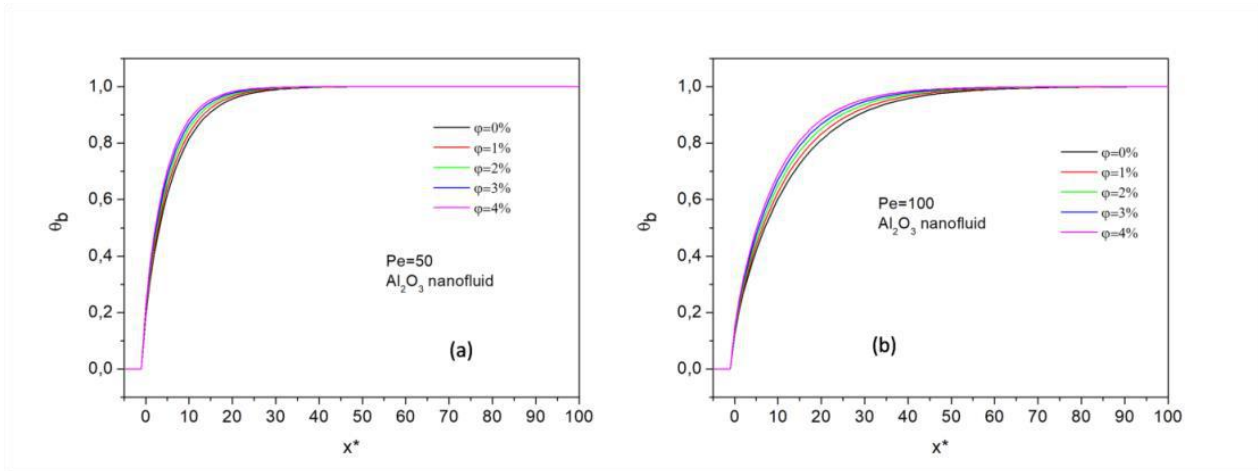


Figure 4. Axial distribution of fluid bulk temperature a) $Pe=50$ b) $Pe=100$

Furthermore, to verify that the solutions are grid independent, results were assessed based on the generalized Richardson extrapolation and grid converge index (GCI), suggested by [27]. Sample solutions were made by using coarse (80x30) and fine grids(320x120) assuming the selected grid system as medium (160x60). A second order method is used in GCI analysis by taking the grid

refinement ratio as 2.0. The quantity of interest for the comparison is the fluid bulk temperature θ_b , heat flux, q_w^* and Nusselt Number, Nu , at the beginning of the heating section, $x^*=0$. The parameter values used for calculations and the results of GCI analysis are given in Table 3. The computations may be assumed within the asymptotic range and no further refinement is necessary.

Table 3. Effect of grid size on θ_b , q_w^* and Nu

values at $x^*=0$	axial grid		radial grid	fluid bulk temperature (θ_b)	heat flux , q_w^*	Nusselt Number, Nu
	upstream region	down-stream region				
$Pe=50, \phi=0\%$						
fine grid	80	280	120	0.189050	4.6496745	9.9644497
medium grid	40	120	60	0.193015	4.6542981	10.023364
coarse grid	20	60	30	0.201861	4.6921733	10.216929
ϵ between medium and coarse grids (%)				0,018945467	0,00807	0,04382
GCI between medium and coarse grids (%)				1,036172723	0,140301	4,449492
ϵ between fine and medium grids (%)				0,005877726	0,00099	0,02054
GCI between fine and medium grids (%)				0,321466841	0,017267	2,085692

IV. RESULTS AND DISCUSSION

The problem handled depends on Peclet number, Pe , and volume fraction of nanoparticle Al_2O_3 -water and For different volume, fractions are considered. Solutions are

made for $Pe= 20, 50$ and 100 and $j=1\%, 2\%, 3\%$ and 4% . The volume fraction values are chosen at the limit value of single phase solution. Results are given by heat flux values, fluid bulk temperature values and local Nusselt number

values. The dimensionless distance is $L_h^*=24$ for whole solutions. Also the space (unheated lengths) is equal to 24. In the figures the heated axial distances are presented since the rest of the downstream is assumed as unheated.

In Figure 5, variations of surface heat flux values for $Pe=20$, 50 and 100 are given for four different volume fractions of nanofluid. In this figure, positive and negative heat flux values can be seen. The positive heat flux values correspond to heated sections of the parallel plate. The locations without heater of the wall show negative interfacial heat fluxes due to lower fluid temperature than to the wall. The effect of axial conduction cannot be seen due to the high Peclet number since there is not any heat penetration to the upstream region. As can be seen from Fig.5, as the Peclet numbers increases the heat flux values increases.

The effect of volume fractions of nanoparticles can also be seen in Fig.5. The heat flux values are greater for pure water for heated locations.

Volume fractions of nanoparticles do not change the values of heat fluxes significantly. At the locations where the heat is applied the heat flux values decreases as the volume fraction increase. But in the un-heated locations, this phenomenon changes vice versa. In the locations without the heater, the lower values of heat fluxes are for pure water and the values of heat fluxes are increased as the volume fraction increases. The value of heat flux of pure water is lower than the other volume fraction at unheated locations. And as the ϕ increases the heat flux values increases also. From Fig. 5. it can also be seen that the peak values get the same values this can be due to value of heating and unheating lengths. Especially for $Pe=20$ and $Pe=50$ (Fig 5. a and b) the heating and unheated lengths are sufficient for thermal developing but it is not for $Pe=100$. Because of this phenomenon the first peak value of heat flux is slightly greater than others for Fig.5.c.

In Figure 6 distribution of bulk temperatures as axial distance is given. Fig. 6.a, 6.b and 6.c are given for Peclet numbers 20, 50 and 100 respectively. In these figures the heated and unheated lengths are taken as 24 and equals to each others. As can be seen from Figure 6, there is not any heat diffusion through the upstream due to axial conduction in the fluid. In bulk temperature curves the increment trend occurs during the heating location and the decrement trend follows it at the unheated locations. The maximum and minimum values are bounded between 0 and 1. The bulk temperature values are higher for the higher volume fractions at the heated locations of the parallel plate. In the unheated locations, the bulk temperature values get lower values for high volume fraction than the others. This can be explained due to higher thermal conductivity of nanofluids.

The thermal conductivity increases as the volume fraction increases.

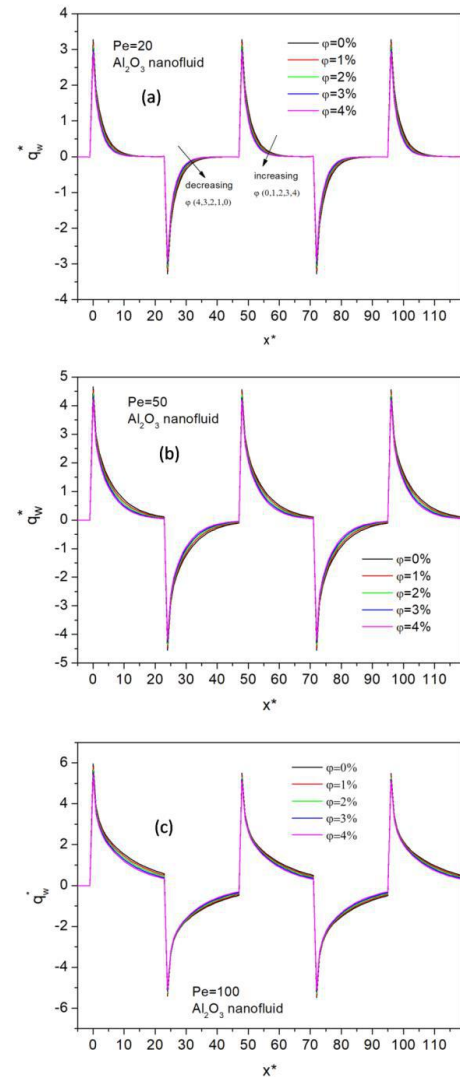


Fig.5. Variation of surface heat flux. a) $Pe=20$, b) $Pe=50$ c) $Pe=100$

As can be seen from Fig. 6.a, the bulk temperature gets its limit value of 1 at a short distance than the heated sections. This is also seen for unheated sections. In these locations the value gets its value of 0. This can be explained by the slow motion of the fluid in parallel plate. The effect of volume fractions of nanofluids cannot be seen at lower Peclet numbers distinctly. The curves of volume fractions get clear as the Peclet numbers increases. The smaller Peclet number indicates slower fluid flow in the channel. As the Peclet number decreases the differences between bulk temperature curves of nanofluid decreases due to higher fluid conduction.

As can be seen from Fig. 6.c, at downstream region the peak values of bulk temperatures move away from boundary

values The top value is nearly 0.9 and the bottom bulk temperature value is 0.05. The rapid fluid motion causes this difference. The effects of volume fractions of nanoparticles are more significant at higher Pe numbers.

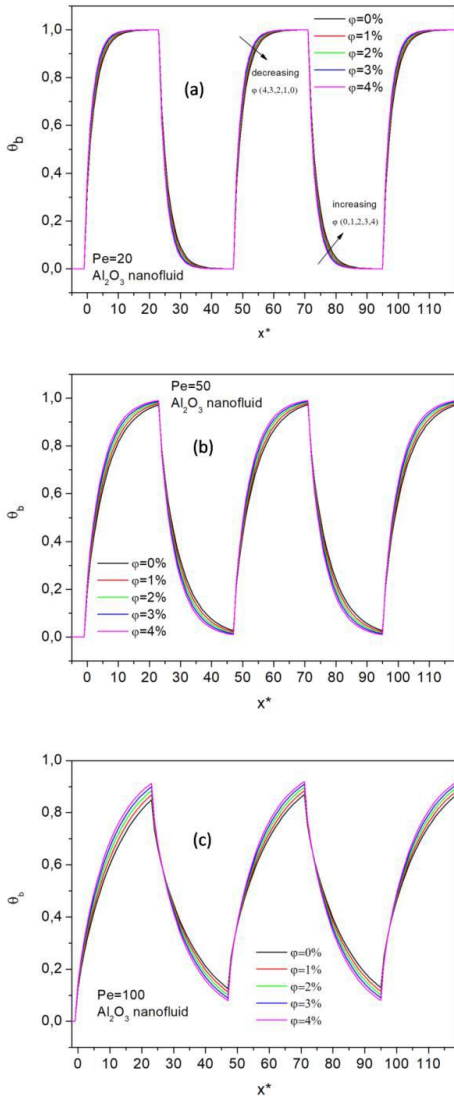


Figure 6. Axial distribution of fluid bulk temperature. a)Pe=20, b)Pe=50 c)Pe=100

Figure 7 shows the local Nusselt number values for the downstream section of the parallel plate. Fig. 7.a, 7.b and 7.c are given for Pe=20, 50 and 100 respectively. As can be seen from Fig. 7 at the vicinity of heating section Nusselt numbers get their maximum value and asymptotically decrease to a limit value at each un-heated locations. The effects of volume fractions are clearer in these three figures. At each Nusselt graphics, the minimum values are for the pure water ($\phi=0\%$). the Nusselt number values increase as the volume fraction of nanofluid increases.

From Fig.7 it can also be seen that the values of Nusselt numbers are greater for greater Peclet numbers. The local Nusselt number values increases as the Peclet number increases. This result is coherent with the results of Fig.6, since the differences of bulk and wall temperatures are higher at higher Peclet numbers. The temperature difference is at the denominator of Eq. 7.

As can be seen from Fig.7.a. by using 4% of nanofluid the Nusselt number increases up to 25% for Pe=20. From Fig. 7.b this percentage is up to 30% for Pe=50, and from Fig.7.c it is 30% for Pe=100 than to pure water. Similar Nusselt number increment ratios are also obtained for four different volume fractions for classical heat transfer problem. This can be seen by comparison of Fig.3 and Fig. 7. This result is coincident with the result of Huang (2015). The results show that the Nusselt numbers of Al₂O₃-water nanofluids are significantly higher than that of base fluid because of their higher thermal conductivity.

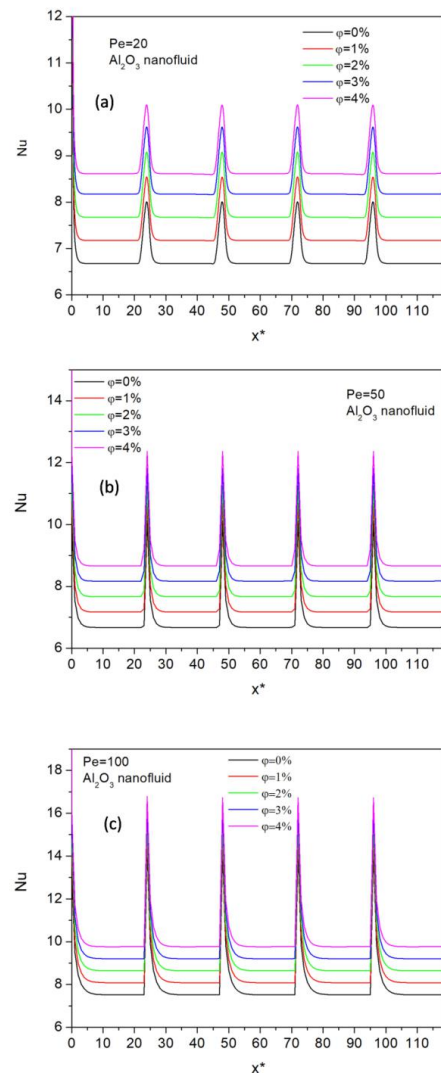


Figure 7. Local Nusselt numbers a)Pe=20, b)Pe=50 c)Pe=100

V. CONCLUSION

This work presents an investigation of heat transfer in a parallel plate heated with flush mounted discrete heat sources with constant surface temperature. The problem is handled for two regional plate, infinite in length, for which the upstream region is completely kept at uniform temperature T_o , which is also the inlet temperature. After $x=0$, flush mounted six heaters at temperature T_1 placed at the top and bottom plates (three for top and three for bottom) with same spaces while the rest of the system kept at T_o . The solution is made numerically by a finite difference method for hydrodynamically developed laminar flow. Al_2O_3 -water is assumed as flowing through the parallel plates. The effects of volume fractions of nanofluid were obtained for four different values varying from 0%-4%. The heat fluxes, bulk temperatures, and Nusselt numbers are obtained for three different Peclet numbers. A classical heat transfer problem, which is heated with constant wall temperature downstream, is solved for the validity of the computer program. And effects of volume fractions are also determined for this problem. The results obtained may be outlined as follows.

- The local Nusselt number values increase as the volume fraction increases as expected due to higher thermal conductivity in the classical heat transfer problem.
- The volume fractions of nanoparticles do not have a significant effect on thermal development length on the classical problem.
- At the locations where heat is applied the heat flux values decrease as the volume fraction increase. And at unheated locations it vice-versa.
- The bulk temperature values are higher for the higher volume fractions at the heated locations.
- The Nusselt numbers of nanofluids are significantly higher than that of base fluid because of their higher thermal conductivity. It can increase the heat transfer by 30% than to pure water.

Nomenclature

a	constant of discretization equation (Eq. 14)
y	normal coordinate
d	width of the channel
u	axial velocity
Pe	Peclet number
k	thermal conductivity
L	length
T	temperature
x	axial coordinate

c_p specific heat at constant pressure

q heat flux

T temperature

Nu Nusselt number

C empirical constant

Subscripts

nf nanofluid

m mean

b bulk

eff effective

h heated length

w wall

f fluid

p particle

φ volume fraction

α thermal diffusivity

μ dynamic viscosity

i,j at nodal point i,j

Superscripts

*Dimensionless quantity

Greek symbols

θ dimensionless temperature

ρ density

δx axial position of difference

δy normal position of difference

Δx axial step size

Δy normal step size

\in quantity in GCI analysis

REFERENCES

- [1] R.K. Shah., and A.L. London, Laminar Flow Forced Convection In Ducts: A Source Book For Compact Heat Exchanger Analytical Data, 1978, Academic Press.
- [2] T. Alves, and C.A.C. Altemani, "Conjugate cooling of a discrete heater in laminar channel flow," Journal of the Brazilian Society of Mechanical Sciences and Engineering, Vol.33 No.3, (2011), pp. 278-286. <https://doi.org/10.1590/S1678-58782011000300003>.
- [3] Q.Wang., and Y. Jaluria., "Instability and heat transfer in mixed-convection flow in a horizontal duct with discrete heat sources," Numerical Heat Transfer, Part A, Vol.42,(2002), pp.445-463. DOI: 10.1080/10407780290059648.
- [4] S. Ramadhyani, D.F. Moffatt, and F.P. Incropera, "Conjugate heat transfer from small isothermal heat sources embedded in a large substrate," International Journal of Heat and Mass Transfer, Vol. 28, No. 10, (1985), pp. 1945-1952.

- [5] R. Sugavanam, A. Ortega, A., and C.Y. Choi, "A numerical investigation of conjugate heat transfer from a flush heat source on a conductive board in laminar channel flow," *International Journal of Heat and Mass Transfer*, Vol.38, No. 16,(1995), pp. 2969-2984., DOI: 10.1109/ITHERM.1994.342913.
- [6] M. A. Hassab, M.K. Mansour, and M.S. Ismail, "The effect of axial wall conduction on heat transfer parameters for a parallel-plate channel having a step change in boundary conditions," *Numerical Heat Transfer, Part A: Applications*, Vol.63, No.6, (2013), pp.430-451, DOI: 10.1080/10407782.2013.742764.
- [7] F.P. Incropera, J.S. Kerby, D.F. Moffatt, and S. Ramadhyani, "Convection heat transfer from discrete heat sources in a rectangular channel," *International Journal of Heat and Mass Transfer*, Vol. 29, No.7, (1986), pp. 1051-1058., DOI: [https://doi.org/10.1016/0017-9310\(86\)90204-8](https://doi.org/10.1016/0017-9310(86)90204-8).
- [8] R. Mathews, and C. Balaji, "Numerical simulation of conjugate, turbulent mixed convection heat transfer in a vertical channel with discrete heat sources," *International Communications in Heat and Mass Transfer*, Vol. 33, No.7, (2006), pp. 908-916., DOI: <https://doi.org/10.1016/j.icheatmasstransfer.2006.02.013>.
- [9] A. Dogan, M. Sivrioglu, and S. Baskaya, "Investigations of mixed convection heat transfer in a channel with discrete heat sources at the top and at the bottom," *International Journal of Heat and Mass Transfer*, Vol. 49, No.15-16 (2006), pp. 2652-2662. DOI: <https://doi.org/10.1016/j.ijheatmasstransfer.2006.01.005>.
- [10] C. Rao, C. Balaji, and S. Vankateshan, "Effect of surface radiation on conjugate mixed convection in a vertical channel with a discrete heat source in each wall," *International Communications in Heat and Mass Transfer*, Vol. 45,(2002), pp. 3331-3347.
- [11] P.M. Guimarães, and G.J. Menon, "Combined free and forced convection in an inclined channel with discrete heat sources," *International Communications in Heat and Mass Transfer* Vol.35, No.10, (2008) pp. 1267-1274. DOI: <https://doi.org/10.1016/j.icheatmasstransfer.2008.08.006>.
- [12] M.A. Mansoura and S.E. Ahmed, "A numerical study on natural convection in porous media-filled an inclined triangular enclosure with heat sources using nanofluid in the presence of heat generation effect," *Engineering Science and Technology, an International Journal*, Vol. 18, No. 3, (2015), pp. 485-495., DOI: <https://doi.org/10.1016/j.jestch.2015.03.007>.
- [13] C.Y. Choi and A. Ortega, "Mixed convection in an inclined channel with a discrete heat source," *1992 Proceedings, Intersociety Conference on Thermal Phenomena in Electronic Systems*, (1992), pp. 40-48, DOI: 10.1109/ITHERM.1992.187739.
- [14] O. Manca, S. Nardini, and D.A. Ricci, "A numerical study of nanofluid forced convection in ribbed channels," *Applied Thermal Engineering*, Vol. 37,(2012),pp. 280-292., DOI:<https://doi.org/10.1016/j.applthermaleng.2011.11.030>[15] İ.O. Sert, N. Sezer-Uzol and S. Kakaç, "Numerical analysis of transient laminar forced convection of nanofluids in circular ducts," *Heat Mass Transfer*, Vol.49, (2013), pp.1405-1417. <https://doi.org/10.1007/s00231-013-1184-1>
- [16] S. Kakaç and A. Pramuanjaroenkij, "Review of convective heat transfer enhancement with nanofluids," *International Journal of Heat and Mass Transfer*, Vol. 52, No.13-14, (2009), pp. 3187-3196., DOI:<https://doi.org/10.1016/j.ijheatmasstransfer.2009.02.006>.
- [17] S. Kakaç and A. Pramuanjaroenkij, "Single-phase and two-phase treatments of convective heat transfer enhancement with nanofluids – A state-of-the-art review," *International Journal of Thermal Sciences*, Vol.100, (2016), pp. 75-97., DOI:<https://doi.org/10.1016/j.ijthermalsci.2015.09.021>.
- [18] A.A. Minea, "A study on Brinkman number variation on water based nanofluid heat transfer in partially heated tubes," *KONA Powder and Particle Journal* No. 32 (2015), DOI:10.1016/j.mechrescom.2016.01.013.
- [19] A. Bahrami, A.H. Poshtiri, and A. M. Akbarpoor, "Nusselt number correlations for forced convection in a microchannel including discrete heat sources," *Journal of Thermophysics and Heat Transfer*, (2019), pp. 1-12. <https://doi.org/10.2514/1.T5814>.
- [20] M. Elahmer, S. Abboudi, and N. Boukadida, "Nanofluid effect on forced convective heat transfer inside a heated horizontal tube," *International Journal of Heat and Technology*, Vol. 35, No. 4, (2017), pp. 874-882.
- [21] D. Wen and Y. Ding, "Experimental investigation into convective heat transfer of nanofluids at the entrance region under laminar flow conditions," *Int. J. Heat Mass Transfer*, Vol. 47, No.24, (2004), pp. 5181-5188., DOI: <https://doi.org/10.1016/j.ijheatmasstransfer.2004.07.012>.
- [22] Y. Xuan and W. Roetzel, "Conceptions for heat transfer correlation of nanofluids," *Int. J. Heat Mass Transfer*, Vol.43, No.19, (2000), pp. 3701-3707., DOI: [https://doi.org/10.1016/S0017-9310\(99\)00369-5](https://doi.org/10.1016/S0017-9310(99)00369-5).
- [23] G.K. Batchelor, "The effect of Brownian motion on the bulk stress in a suspension of spherical particles," *J. Fluid Mech.*, Vol. 83, No.1, (1977), pp. 97-117, DOI: <https://doi.org/10.1017/S0022112077001062>.
- [24] Ş. Bilir, "Numerical solution of Graetz problem with axial conduction," *Numerical Heat Transfer, Part A: Applications*, (1992). Vol.21, No.4, pp.493-500. DOI: <https://doi.org/10.1080/10407789208944889>.
- [25] S. Patankar, *Numerical Heat Transfer and Fluid Flow* (1st ed.), (1980), CRC Press. <https://doi.org/10.1201/9781482234213>
- [26] Y. Huang, "Entry flow and heat transfer of laminar and turbulent forced convection of nanofluids in a pipe and a channel," *Engineering and Applied Science Theses and Dissertations*, (2015) No.112.
- [27] P.J. Roache, "Perspective: A method for uniform reporting of grid refinement studies," *ASME. J. Fluids Eng.*, Vol.116, No.3, (1994), pp. 405-413.,